



<https://doi.org/10.15517/rev.biol.trop..v72i1.56729>

Environmental controls on bioluminescent dinoflagellate density, in Laguna Grande, Fajardo, Puerto Rico

Yogani Govender^{1*};  <https://orcid.org/0009-0006-7216-1075>

Mark R. Jury²;  <https://orcid.org/0000-0002-6871-403X>

1. Climate & Ecological Studies Lab, Interamerican University of Puerto Rico, Metropolitan Campus, San Juan, PR, USA; ygovender@metro.inter.edu (Correspondence*)
2. Physics Department, University of Puerto Rico, Mayaguez, PR, USA; mark.jury@upr.edu

Received 27-IX-2023. Corrected 27-II-2024. Accepted 24-VII-2024.

ABSTRACT

Introduction: Bio bays in Puerto Rico play an important socio-economic role and declines in dominant bioluminescent dinoflagellate *Pyrodinium bahamense* are concerning. Studies show erratic blooms with its weak correlation to *in situ* environmental factors. Our study examines shorter field and longer proxy records on dinoflagellate density at Laguna Grande de Fajardo (LGF).

Objectives: To quantify temporal changes in dinoflagellate density in a long-term monitoring study, understand how the marine environment modulates those changes, and determine the wider impacts of a fluctuating climate and extreme events on proxies for dinoflagellate density.

Methods: Bimonthly samples were collected from 2016 to 2021 at three sampling sites in LGF. Dinoflagellates density was estimated by Sedgewick Rafter counting cells. Environmental conditions were obtained from Rio Fajardo 5007100 station and NOAA buoy 41056. Marine climate and biotic proxies were obtained from remote sensing measurements. Kruskal Wallis, Spearman correlations and cross-correlations in the shorter field and longer proxy records were used to evaluate environmental controls on LGF dinoflagellate blooms.

Results: Six years of field monitoring densities found a low period in 2016-2017, frequent and intense blooms in 2018-2021 punctuated by hurricanes. Generally low values were recorded in late winter in contrast with higher values in late summer (Aug-Nov). Light winds and mixed layer response to seasonal warming in the form of high tides and low salinity, were found to sustain dinoflagellate reproduction.

Conclusions: Bioluminescent dinoflagellates are vital to coastal tourism and require resource management. LGF results show that: 1) dinoflagellate counts fluctuate widely, 2) fluorescing dinoflagellates are sensitive to environmental conditions because of limited seasonality and narrow physiological range, 3) hurricanes play a role by 'raking and refreshing' the coastal lagoon for subsequent biotic reproduction, and 4) intra-seasonal fluctuations of density and proxies relate to air-sea thermodynamic conditions, the salinity budget and sea level.

Key words: bioluminescent dinoflagellates; coastal lagoon; Puerto Rico.

RESUMEN

Controles ambientales sobre la densidad de dinoflagelados bioluminiscentes, en Laguna Grande, Fajardo, Puerto Rico

Introducción: Las bahías bioluminiscentes en Puerto Rico desempeñan un papel socioeconómico importante y disminuciones del dinoflagelado bioluminiscente dominante *Pyrodinium bahamense* son preocupantes. Los estudios muestran proliferaciones erráticas débilmente correlacionadas con factores ambientales locales.



Objetivos: Cuantificar cambios en la densidad de dinoflagelados a largo plazo en la Laguna Grande de Fajardo (LGF), comprender cómo el ambiente marino modula esos cambios y determinar los impactos de eventos climáticos extremos en la densidad de dinoflagelados.

Métodos: Se recolectaron muestras bimestrales del 2016-2021 en tres sitios de la LGF. La densidad se estimó mediante el conteo de células de Sedgewick Rafter. Condiciones ambientales se obtuvieron de la estación Río Fajardo 5007100 y de la boya NOAA 41056. El clima marino y los indicadores bióticos se obtuvieron por mediciones de teledetección. Se utilizaron correlaciones Kruskal Wallis, Spearman y las correlaciones cruzadas en los registros de campo corto y proxy largos para evaluar los controles ambientales en las proliferaciones de dinoflagelados LGF.

Resultados: En seis años de monitoreo se encontraron densidades bajas entre el 2016-2017 y proliferaciones frecuentes e intensas en 2018-2021 marcadas por huracanes. Se registraron valores bajos a finales del invierno, en contraste con valores más altos a finales del verano (agosto-noviembre). Vientos ligeros y la respuesta de capas mixtas al calentamiento estacional en forma de mareas altas y baja salinidad, mantienen la reproducción de los dinoflagelados.

Conclusiones: Los dinoflagelados bioluminiscentes son vitales para el turismo costero y requieren manejo de los recursos. En general: 1) los recuentos de dinoflagelados fluctúan ampliamente, 2) los dinoflagelados fluorescentes son sensibles a las condiciones ambientales debido a su estacionalidad limitada y estrecho rango fisiológico, 3) los huracanes juegan un rol de rastrear y refrescar la laguna costera para su posterior reproducción, y 4) fluctuaciones intra-estacionales se relacionan con las condiciones termodinámicas aire-mar, el balance de salinidad y el nivel del mar.

Palabras clave: dinoflagelados bioluminiscentes; laguna costera; Puerto Rico.

INTRODUCTION

While dinoflagellates around the world are associated by harmful algal blooms (HAB's) (Badylak & Phlips, 2009; Morquecho, 2019), in Puerto Rico, the bioluminescence of the dominant species *Pyrodinium bahamense* has resulted in a lucrative eco-tourism industry. Bioluminescent bays of Puerto Rico include Laguna Grande de Fajardo on the Northeastern tip, Mosquito Bay on the offshore island of Vieques, and La Parguera on the Southwestern coast (Bahía Fosforescente). They are surrounded by nature reserves under the Department of Environment and Natural Resources (DNER, 2013), managed to protect the fringing mangroves, access channels, water quality, and stimulate adventure tourism (Weaver et al., 1999). Commercial tour operators reported ~34 000 kayaks rented to visit Laguna Grande in 2018 earning approximately \$1.7 million (DNER, 2013). Due to the socio-economic benefits of the dominant bioluminescent dinoflagellate *P. bahamense*, numerous impact assessments for bio bays have been made. Sustained blooms involve a delicate balance of environmental conditions that control the flux of nutrients and

biological uptake (O'Connell et al., 2007). Their density fluctuates over months and years due to flushing action around the coastal lagoon's fringing coral reefs and mangrove vegetation, controlled by sea level, wind-driven currents and waves, sunlight and turbidity, sea temperatures in the range 24-29 °C, salinity, run off and organic content (Sastre et al., 2013; Soler-López & Santos, 2010).

At La Parguera Puerto Rico, Soler-Figueroa & Otero (2014) and Soler-Figueroa & Otero (2016) measured sea temperature, salinity, nutrient concentration, rainfall, wind velocity, and dinoflagellate count at multiple sites during wet and dry seasons. In the wet season (Aug-Nov), they found *P. bahamense* abundance increased under warmer sea temperature and lower salinity. Sastre et al. (2013) studied dinoflagellates at Laguna Grande Fajardo (hereafter: LGF) and found higher *P. bahamense* densities in summer and lower densities in winter (Dec-Mar), but erratic fluctuations of *Ceratium (Tripos) furca*. They found weak correlations between dinoflagellate density and the in-situ marine environment and nutrients (phosphate, nitrate), except for a negative correlation between fluorescence and salinity.

LGF is surrounded by a nature reserve on the Northeast tip of Puerto Rico, with a depth of 3 m (Soler-López & Santos, 2010) and mean annual rainfall ~1 500 mm. Freshwater runoff to LGF is sporadic and secondary to seawater exchange, especially during high tides from August to November. The freshwater flux is confined to infrequent storms and does not represent an effective water-renewal mechanism for LGF. Yet floods and drought do alter salinity, sea temperature, and pH (Sastre et al., 2013; Soler-López & Santos, 2010).

The loss to tourism-related businesses due to the 2018 Florida HABs was estimated to be \$2.7 billion USD (Alvarez et al., 2024), which implies that HABs and their impact on eco-tourism can be considered as a potential 'billion-dollar' disaster for bio bays in Puerto Rico. In 2003 and 2013, low seasons of bioluminescence raised public and ecological concern (Pagán, 2021; Xei, 2013). The DNER (2013) attributed the decreases to lower sea-level/runoff/nutrients in the ecosystem. Conversely, shifts in marine climate resulting in increased storm events and hurricanes have caused significant shifts in dinoflagellate communities and density in Florida (Fiorendino et al., 2021; Lopez et al., 2021; Philips et al., 2020). Thus, our study of ocean influences during an active hurricane season on dinoflagellates in LGF was conceived to 1) Quantify temporal changes in bioluminescent dinoflagellate density in a six year monitoring study, 2) Understand how the marine environment modulates those changes, and 3) Determine the wider impacts of a fluctuating climate and extreme events on proxies for dinoflagellate density over two decades.

MATERIAL AND METHODS

Dinoflagellate sampling points were established in LGF: Pt.1 in Southwest shallows (0 m depth), pt.2 in the Middle (2 m depth), pt.3 in mid-Northern shallows (0 m), and pt.4 (from 2018) at the Southeast canal entrance (Fig. 1A, Fig.1B, Fig. 1C). Each point was sampled twice a month from July 2016 to December 2021 just after sunset 19:00 + LST, so to observe

bioluminescence on a 0-3 scale: None-to-high. LGF watercolor ranged from 0: dark, 1: pale white, 2: blue hue, 3: bright turquoise, with 1 and 2 requiring water stirring. In addition to such visual observations, three 1 l water samples were collected by hand in the shallows, and with a Van Dorn depth sampler at point 2 (at 2 m). Sampling was disrupted from Oct-Dec 2017 by hurricanes and Mar-Apr 2020 by the COVID-19 pandemic. Water samples were preserved with 20 ml of 2 % formalin and transported to the Climate & Ecological Studies Lab at the Interamerican University of Puerto Rico, San Juan.

Organisms settled to the bottom of the 1 l bottle (Huber, 2012) and were marked by a line at 20 ml. The remaining water was decanted after 48 hours using an automated 100 ml volumetric pipette and filtered through a 20 μ m Nitex nylon mesh to isolate phytoplankton in suspension (Sastre et al., 2013). The unfiltered 20 ml sample and cells retained by the mesh were combined, washed into a 50 ml Falcon centrifuge tube, and stored in our lab. The concentrated plankton samples were swirled in a 50 ml tube for counting, and a 1 ml subsample was transferred to a gridded Sedwick-Rafter (S-R) (Huber, 2012). The S-R counting cell was covered with glass, and all identifiable dinoflagellate taxa were counted using a Leica CME or Nikon Eclipse microscope at 100-200X magnification.

Since Sastre et al. (2013) found little correlation between the lagoon environment and dinoflagellate density, open ocean data were collected from a NOAA buoy 41056: 18.26°N & 65.46°W (CariCOOS, 1996). Time series were obtained during the field monitoring for wind velocity, air and sea temperature and salinity. Fresh water inputs to LGF were derived from U.S. Geological Survey (2021) river discharge at Rio Fajardo 5007100. Using ~ 66 months of environmental data, a statistical analysis was conducted by averaging bioluminescent dinoflagellate density in LGF to monthly. Comparative work employed the non-parametric Kruskal Wallis and Tukey Tests, Spearman cross-correlation and multi-variate regression.

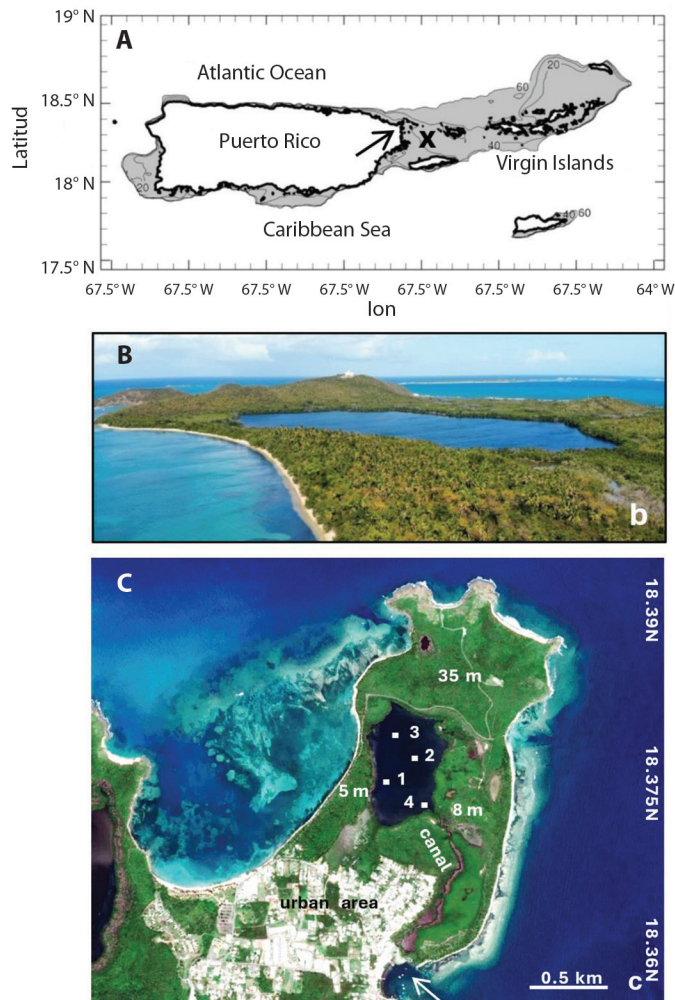


Fig. 1. A. Puerto Rico's coast with shelf 0-60 m shaded; arrow points to LGF, buoy = x. B. Aerial view of LGF from SW to NE. C. Close-up of Fajardo Peninsula and the coastal lagoon, sampling points, elevation labels, canal exchange with ocean denoted by arrow.

The non-parametric tests were used because dinoflagellate density did not meet the normality assumption even after attempts of transformation. The Kruskal Wallis Test and Tukey Test is used to compare dinoflagellates density by month, year, and sampling station. Correlation analysis was completed for wind direction, wind speed (m/s), air pressure (hPa), marine air temperature (°C), salinity (‰), sea temperature (°C), Fajardo River discharge (ft³/s) and dinoflagellate density (ind/l).

After review, a second independent analysis was conducted over a wider area and longer period 2002-2022 using satellite and coupled reanalysis fields based on assimilation of in-situ and remote sensing measurements (Balmaseda et al., 2015; Storto et al., 2019). Daily time series were extracted at LGF: 18.39°N & 65.61°W, and maps of the surrounding marine climate were constructed. MODIS and VIIRS 4 km resolution satellite color radiance around LGF (Fig 1B) was extracted in the form of green-band

chlorophyll (0.44 μm) and red-band fluorescence (0.67 μm). Other satellite data sets include satellite visible-band 4 km land vegetation color fraction, infrared 4 km GHR sea surface temperature (SST), 25 km resolution EC multi-satellite altimeter sea level, net outgoing longwave radiation (OLR) to represent atmospheric convection, and MODIS radiometer light extinction by atmospheric dust. The Hybrid Coordinate Ocean Model 10 km resolution coupled reanalysis (HYCOM3), (Chassignet et al., 2009) described surface ocean currents, salinity, mixed layer depth (MLD) and Ekman transport. Wavewatch 3 (W3) 25 km reanalysis (Tolman, 2002) was used for surface wave characteristics, based on buoy and satellite assimilation in a multi-spectral model (Chawla et al., 2013).

Marine weather at LGF was characterized by 25 km resolution European Reanalysis (ERA5) and NOAA Coupled Forecasts (CFS2) (Hersbach et al., 2020; Saha et al., 2014) for surface winds, total heat balance and net solar radiation. Environmental impacts of the 2017 hurricanes were studied via hourly gauge sea level, buoy SST, daily wind time series and satellite vegetation color fraction. Currents and salinity were analyzed for 2018-2019 during dinoflagellate blooms in LGF, as Hovmöller plots on a N-S slice 65.6W in 2018-2019, and as maps for 10 Oct. 2019 and 9 Nov. 2020.

Within the longer records, we found that satellite red-band radiance (Jury, 2020) was out-of-phase with our field data, so it was relegated. Instead satellite green-band chlorophyll aligned with dinoflagellate counts, while environmental conditions were represented by sea level and salinity. Pair-wise cross-correlations with satellite and reanalysis variables (cf. Table 4) were

calculated to establish environmental influences over 2002-2022 and 2016-2021 respectively. Serial persistence limits the degrees of freedom so $|R| > 0.20$ (longer record) and > 0.38 (shorter record) reaches 98 % confidence. To understand inter-annual climate influence, 20 year time series were filtered to remove cycles below 18 months (de-seasonal). Detrended cross-correlations were analyzed for sea level, zonal wind, and salinity. Wavelet spectra were calculated to determine significant periodicity. Late summer (Aug-Nov) chlorophyll content was regressed onto fields of ERA5 surface wind, satellite SST and meridional currents around Puerto Rico 14.5-22°N & 70-60°W in the period 2002-2022.

Point measurements from buoys, gauges and stations should be supplemented with coastal weather and ocean fields over a longer time to fully explain the environmental controls on bioluminescence in a coastal lagoon. These methods distinguish our work from most field studies with narrow sampling windows confined to in-situ measurements.

RESULTS

Characteristics of field data: Field data (Table 1, Table 2, Fig. 2A) exhibit wide fluctuations of dinoflagellate density in LGF, with monthly counts ranging from 4 388 cells/l in Jun 2018 to $2.19 \cdot 10^6$ cells/l in Nov 2019. Statistical tests quantify the large intra-seasonal variability: Kruskal Wallis: $H = 105.43$, $P < .001$ (Table 3, Fig. 2B). Annual dinoflagellate minima/maxima were noted in the cool dry / warm wet season. Densities were low in 2016-17 compared with 2018-20 (Fig. 2C), yielding significant inter-annual variability (Kruskal Wallis:

Table 1
Descriptive statistics of dinoflagellate density (ind/l) by month 2016-2021 at LGF.

	Jan	Feb	Mar	Apr	May	Jun	Jul	Aug	Sep	Oct	Nov	Dec
Mean	262 523	306 823	334 224	77 687	78 500	302 931	144 706	690 132	379 409	831 808	1 062 000	736 072
Std. Dev.	380 777	321 594	416 978	63 775	91 233	548 597	280 487	797 234	620 360	915 352	940 367	588 353
Min.	15 667	17 944	5 474	36 727	22 556	4 833	7 328	10 000	23 556	142 278	31 000	128 000
Max.	701 050	629 300	877 300	151 167	183 778	1 124 000	646 250	1 654 000	1 475 000	2 160 000	2 190 000	540 000



Table 2
Descriptive Statistics of dinoflagellate density by year at LGF (months sampled).

	2016 (6)	2017 (9)	2018 (11)	2019 (12)	2020 (10)	2021 (10)
Mean	135 425	41 559	538 557	781 167	513 659	287 464
Std.Dev.	235 878	48 196	795 056	665 465	468 503	237 243
Min.	7 328	5 474	4 833	22 556	29 950	103 301
Max.	598 390	151 167	2 176 000	2 200 000	1 591 000	857 000

Table 3
Tukey test to compare dinoflagellate density by month.

Months	Months	Mean Diff.	SE	t	P _{tukey}
1	11	-817 016	168 621	-4.845	< .001
2	11	-729 254	161 995	-4.502	< .001
3	10	-567 362	163 138	-3.478	0.026
3	11	-822 945	162 654	-5.059	< .001
4	8	-610 321	174 368	-3.5	0.025
	10	-748 680	180 020	-4.159	0.002
	11	-1.004e+6	179 582	-5.592	< .001
	12	-655 815	179 582	-3.652	0.015
5	8	-604 420	176 914	-3.416	0.032
	10	-742 779	182 487	-4.07	0.003
	11	-998 362	182 055	-5.484	< .001
	12	-649 914	182 055	-3.57	0.019
6	10	-529 537	159 435	-3.321	0.044
	11	-785 120	158 941	-4.94	< .001
	12	-436 672	158 941	-2.747	0.205
7	8	-538 008	143 392	-3.752	0.01
	10	-676 367	150 213	-4.503	< .001
	11	-931 951	149 688	-6.226	< .001
	12	-583 502	149 688	-3.898	0.006
8	10	-359 182	156 738	-2.292	0.483
	11	-614 765	156 234	-3.935	0.005
9	11	-614 765	156 234	-3.935	0.005

P-value adjusted for 11 degrees of freedom.

H = 182.26 P < .001). Spatial heterogeneity between collection sites in the 50-ha saltwater coastal lagoon was significant (Kruskal Wallis: H = 33.05, P < .001) (Table 4, Fig. 2D).

Comparison with in-situ environmental variables: Discharge and buoy data time series tended to have skew distributions requiring non-parametric tests. Marine environmental conditions off Fajardo (Fig. 3A, Fig. 3B, Fig. 3C, Fig. 3D, Fig. 3E, Fig. 3F) exhibited noteworthy

seasonality: lowest air pressure, weakest average winds; warmest air and sea temperatures and lowest salinity all occurred in the Aug-Nov period. River discharge exhibited large inter-annual fluctuations (Tukey Test: T > 2.3 P < 0.05) unrelated to offshore salinity. Throughout 2016 and early 2017 salinity was high, then declined in 2018 and remained low in subsequent years. Most marine environmental variables were poorly correlated with dinoflagellate density in LGF (Table 5), except salinity

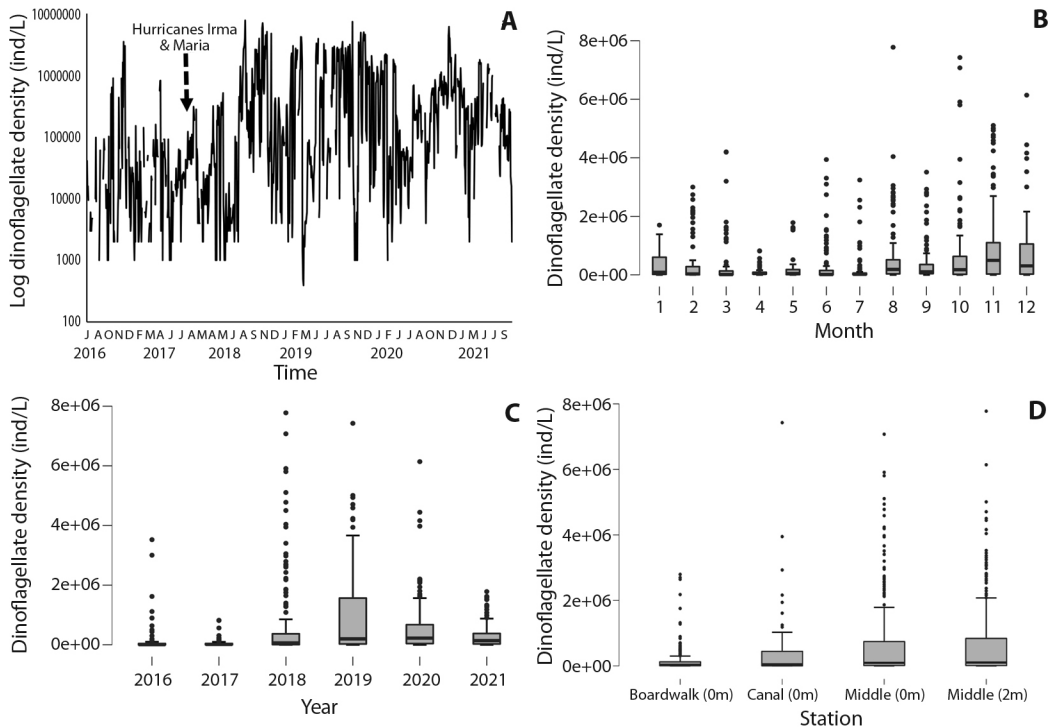


Fig. 2. Variability of dinoflagellate density over six year sampling period by: **A.** Time series of twice-monthly in-situ dinoflagellate density at LGF. **B.** Month. **C.** Year. **D.** Station. Box-whisker plots with median, upper/lower quartiles and outliers.

Table 4

Tukey Test comparison of dinoflagellate density by sampling site.

Station	Mean Diff.	SE	t	P _{Tukey}
1 2	-512 391	85 151.3	-6.017	< .001
1 3	-496 792	85 151.3	-5.834	< .001
1 4	-482 426	165 677	-2.912	0.019
2 3	15 599	85 230.2	0.183	0.998
2 4	29 965	165 717	0.181	0.998
3 4	14 366	165 717	0.087	1

P-value adjusted for 4 degrees of freedom.

(R -0.56), explaining 1/3 of variance (Fig. 4A). Salinity adjustments within LGF may be related to runoff, but current advection may control open ocean conditions (Fig. 4B).

Wider context with satellite reanalysis data: Mapping the long-term average marine conditions Fig. 5A, Fig. 5B and Fig. 5C we find

HYCOM3 salinity gradients between Atlantic 35.9 ‰ and Caribbean 35.4 ‰ waters. Currents sweep Southwestward through the Virgin Islands and turn Northwestward 0.1 m/s near Fajardo. Satellite SST are warmer in the Caribbean (28 °C), leeward of the Antilles Islands. Trade winds prevail at ~ 6 m/s and induce Ekman transport that draws seawater Northward off Fajardo. Time series of daily sea level (Fig. 6A) show rising trends and annual cycling that crests in late October. Higher tides are evident in 2012, 2014, 2015, 2018, 2019, 2021, that tend to flush LGF. Time series of daily SST and salinity (Fig. 6B) show a delayed inverse relationship: warmer sea temperatures are followed by lower salinity. SST shows little trend, while salinity at Fajardo declined after the drought in 2015 and salty spell of 2016-17. Salinity below 34.5 ‰ was evident during late summer (Oct-Nov) of 2019-22, due to an influx of South

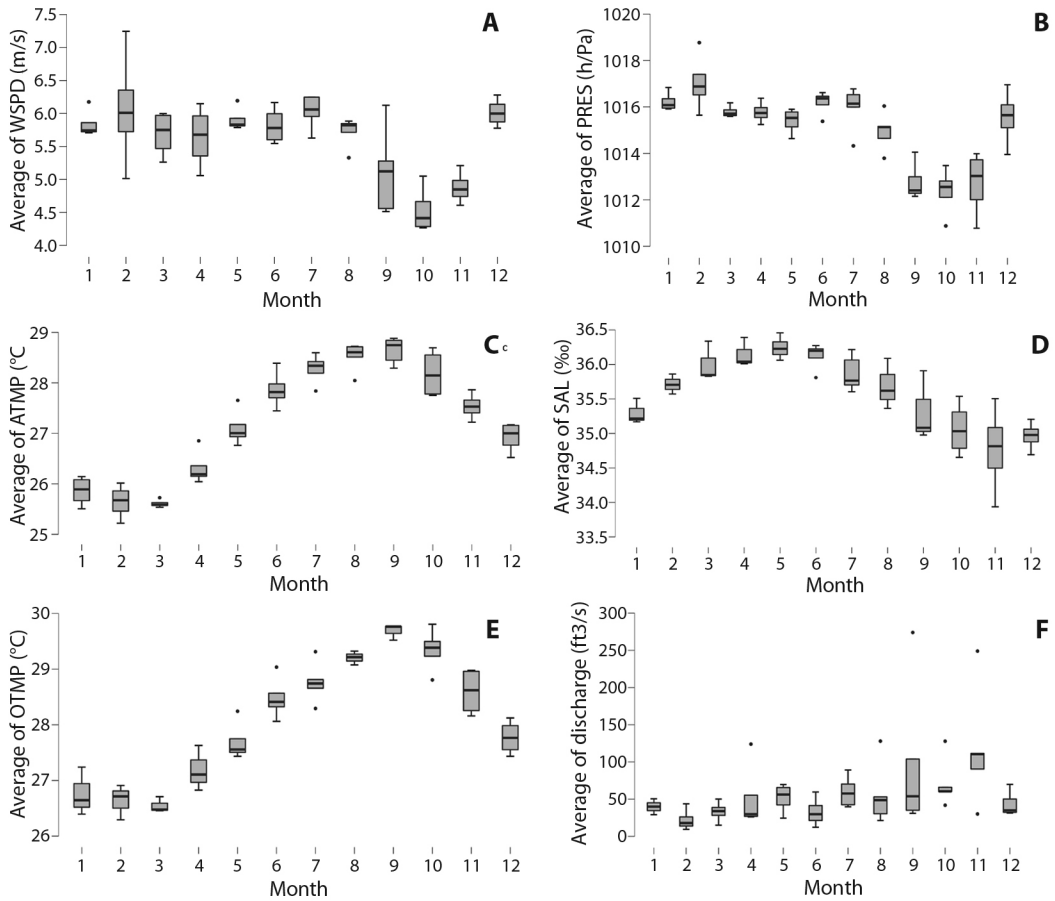


Fig. 3. Box-whisker plots (median, quartiles, outliers) indicating seasonal cycles and inter-monthly variability of: **A.** Wind speed (m/s). **B.** Air pressure (hPa). **C.** marine air temperature (°C). **D.** salinity (‰). **E.** Sea temperature (°C). **F.** Fajardo River discharge (ft³/s).

Table 5

Correlation of Fajardo discharge and buoy time series with monthly dinoflagellate density 2016-2021.

Variable	Spearman Coefficient	Dinoflag. (ind/l)	WDIR (°)	WSPD (m/s)	WGST (m/s)	Pressure (hPa)	airTemp (°C)	seaTemp (°C)	Salinity (‰)
WDIR	R-value	-0.218	-0.538						
	P-value	0.15	< .001						
Pressure	R-value	-0.204	-0.466	0.625	0.619				
	P-value	0.179	< .001	< .001	< .001				
airTemp	R-value	0.113	0.043	-0.306	-0.337	-0.552			
	P-value	0.461	0.763	0.029	0.016	< .001			
seaTemp	R-value	0.121	0.095	-0.417	-0.445	-0.635	0.979		
	P-value	0.451	0.557	0.008	0.004	< .001	< .001		
Salinity	R-value	-0.559	0.028	0.278	0.231	0.305	-0.139	-0.212	
	P-value	< .001*	0.864	0.083	0.151	0.056	0.392	0.172	
Discharge	R-value	-0.068	0.030	-0.056	-0.047	-0.384	0.309	0.328	-0.097
	P-value	0.644	0.833	0.697	0.742	0.006	0.028	0.032	0.534

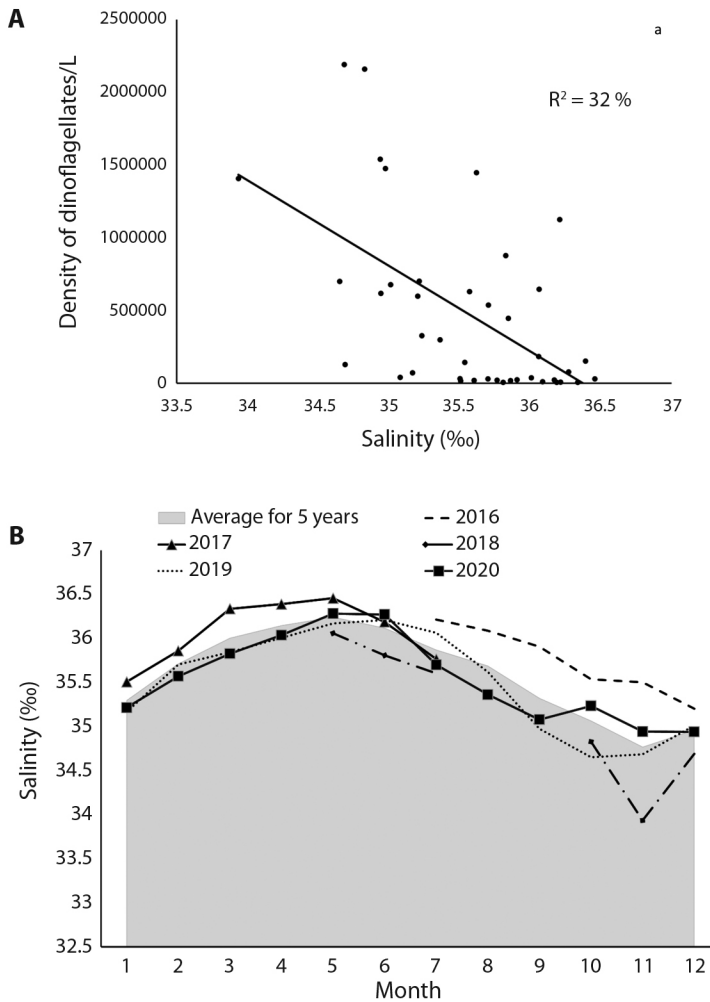


Fig. 4. A. Regression of buoy salinity and dinoflagellate density at LGF. **B.** Temporal cycles of salinity during the monitoring period, lines indicate monthly salinity per year, shaded is the average.

American river plumes. Time series of daily winds and waves (Fig. 6C) are pulsed by tropical cyclones and trade wind surges. Over the 20-year period, 2014-16 had low waves while 2004-10 and 2019-22 saw high wave heights. Although hurricanes generate peak events at Fajardo (Sep 2017), wave action along this coast is diminished by upstream islands and shallow bathymetry.

Turning our attention to seawater color, the satellite green-band radiance (CHLa) map

for Oct 2019 is illustrated in Fig. 7A. High values hug the coast around LGF, and in leeward zones of the Virgin Islands and Puerto Rico. Mean annual cycles are investigated in Fig. 7B, Chlorophyll rises from Jul-Nov (warm wet season) and reaches a minimum in Jan-Apr (cool dry season). Northward currents are bi-modal and peak in summer and winter as trade winds induce Ekman transport. Sea level dips in Mar-Apr and crests broadly from Aug-Nov during infiltration of South American river plumes.

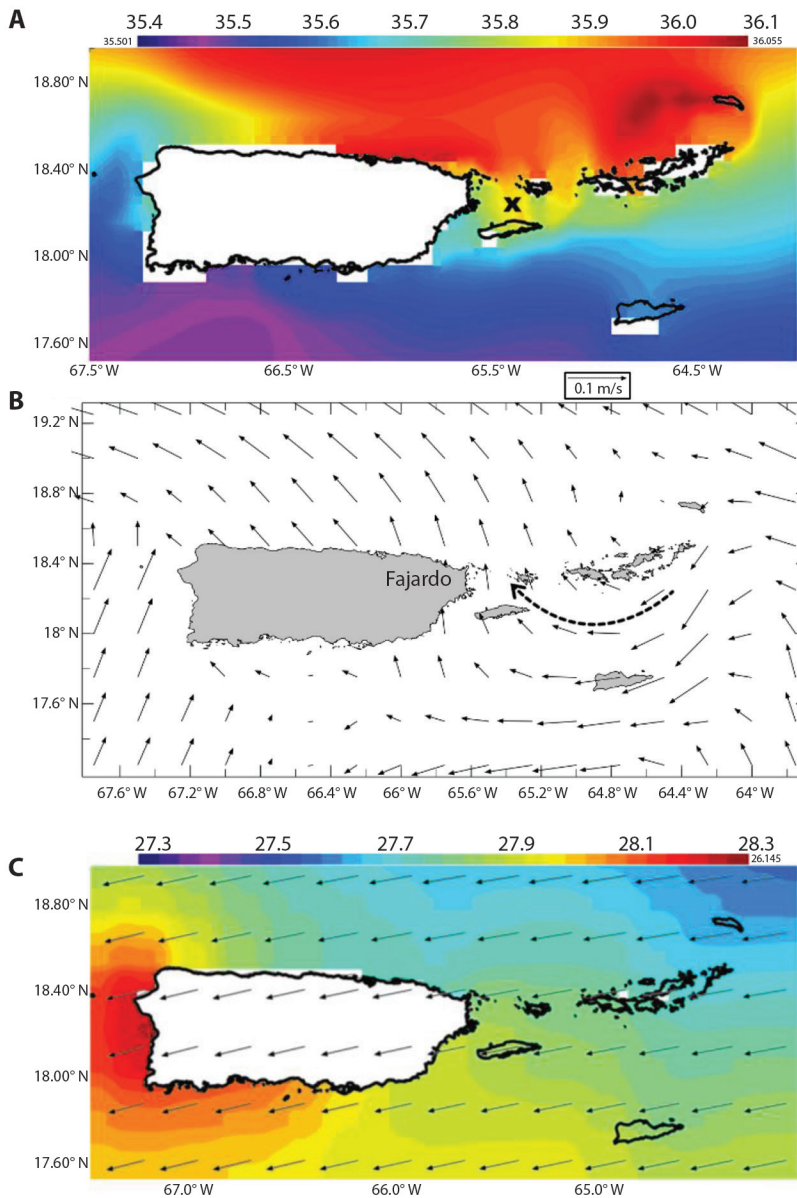


Fig. 5. Long-term mean maps of: **A.** HYCOM surface salinity (‰). **B.** Surface currents (largest 0.1 m/s), dashed arrow highlights inflow. and **C.** GHR satellite sea surface temperature and ERA5 winds (largest vector 7 m/s).

Monthly satellite chlorophyll time series and LGF dinoflagellate counts are plotted in Fig. 7C. The green-band radiance shows high values in 2004, 2009-10, and low values from 2012-2017 that correspond with LGF data. Sustained high chlorophyll content in 2019-2022 coincides with dinoflagellate density above $10^6/l$.

Pair-wise cross-correlations of the Fajardo chlorophyll time series with continuous monthly satellite reanalysis variables 2002-2022 (A) (Table 6) reveals significant associations with SST, atmospheric convection (net OLR) and land vegetation color which reflect how seasonal warming enhances Aug-Nov rainfall

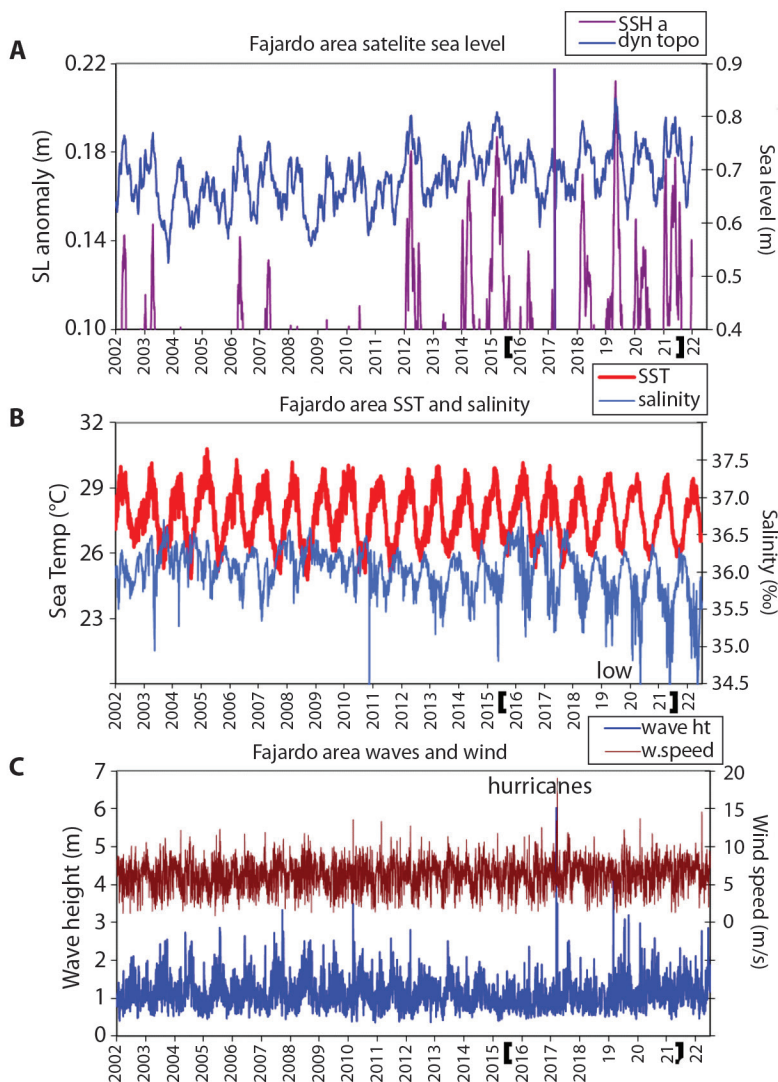


Fig. 6. Daily time series of **A.** Sea level and anomalous high tides at Fajardo, **B.** SST and salinity, and **C.** Wind speed and wave height, identifying key features and storm events, field monitoring bracketed, annual tick marks in July.

and canopy growth. The cross-correlation of LGF dinoflagellates with most environmental variables is weak (B) (Table 6), only sea level is significantly associated, followed by vegetation, solar radiation and salinity. Although satellite chlorophyll and in-situ dinoflagellate counts are weakly associated, they share relationships with many environmental variables.

With sea level being significantly correlated with bioluminescent algal blooms at LGF,

it is inferred that flushing action by high tides in Aug-Nov is beneficial. However, extreme mechanical stress during storm surges may not be. Having earlier noted high dinoflagellate counts in late 2018 and 2019, we focus on environmental conditions during that era by analysis of salinity and currents.

A case of Northward currents and low salinity is mapped in Fig. 8A. This pattern coincides with bioluminescent dinoflagellate

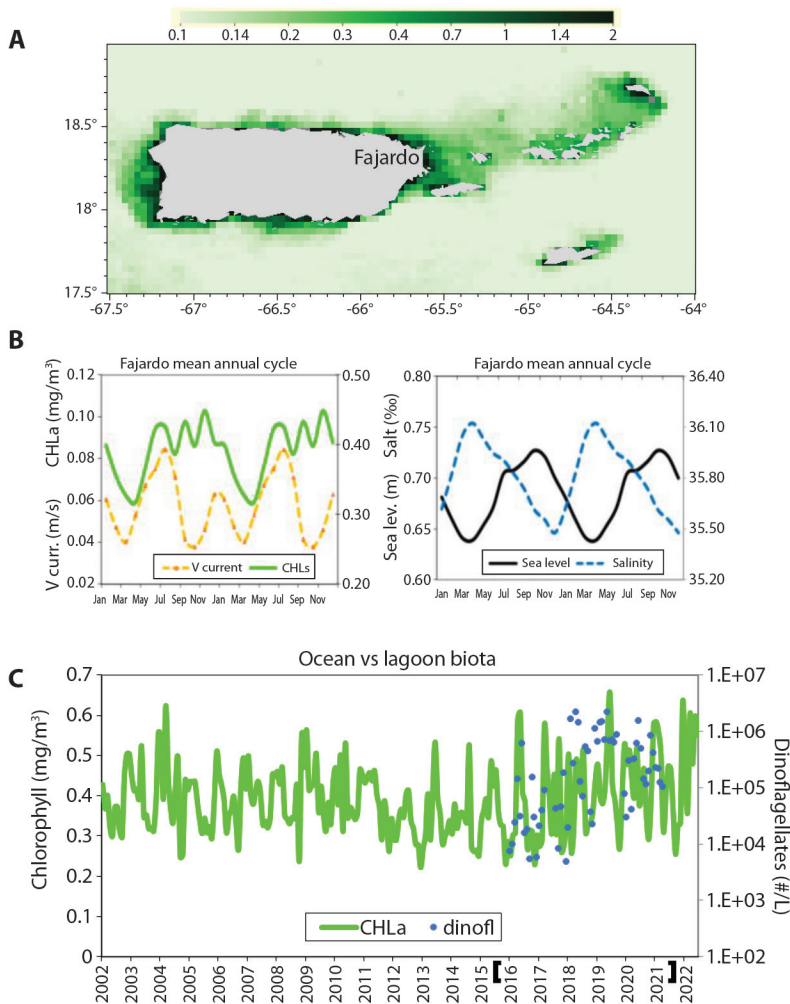


Fig. 7. A. VIIRS satellite chlorophyll map for Oct 2019 (mg/m^3) when blooms were recorded in LGF. **B.** Mean annual cycle of chlorophyll and Northward currents (left) and sea level and salinity. **C.** Time series of CHLa at Fajardo 2003-2022, field monitoring bracketed on y-axis, annual tick marks on July. (CHLa and salt use right-hand axes in b).

blooms in LGF. Currents in the Atlantic sector is Eastward and decline near Fajardo, where they meet Northward currents coming from the Caribbean sector. A strong salinity gradient is sustained. The canal connecting LGF with the open ocean faces the Caribbean and thus entrains low salinity seawater. Dinoflagellate density during this time reached 5-7 million /l. A hovmoller plot of salinity along the East coast (Fig 8B) shows that pulses of low salinity from the Caribbean in Aug-Nov in 2018 and 2019. Surplus precipitation over evaporation and the

Northward spread of river plumes from South America account for these changes.

Analysis of inter-annual variability: To understand inter-annual variability, the 20 year records of Fajardo Sea level, wind and salinity were filtered for oscillations above 18 months. Fig. 9A, Fig. 9B and Fig. 9C illustrate time series that exhibit some coherence. Simultaneous cross-correlations between sea level and salinity are -0.74 and between sea level and U wind -0.59. These outcomes say that increased

Table 6

Cross-correlation of: A. Monthly green-band radiance (CHLa) at Fajardo and marine climate variables from coupled reanalysis 2002-2022, B. Correlation of monthly dinoflagellate density and the same variables 2016-2021.

A	CHLa		CHLa	B	Dinoflag.		Dinoflag.
MLD	-0.13	U wind	-0.06	MLD	0.01	U wind	0.06
salinity	-0.11	V wind	0.09	Salinity	-0.24	V wind	-0.03
SST	0.27	Waves	0.18	SST	0.15	Waves	0.09
U curr	0.18	net heat	-0.09	U curr	0.16	net heat	-0.13
V curr	0.05	Euph Z	-0.19	V curr	-0.04	Euph Z	-0.12
sea level	0.17	dust	0.17	sea level	0.4	dust	-0.18
net OLR	-0.27	Ek V	-0.05	net OLR	0.06	Ek V	-0.22
Veget	0.36	solar	-0.19	Veget	0.27	solar	-0.26
						CHLa	0.15

Bold values have $P < .02$; acronyms: MLD mixed layer depth, SST sea surface temp, U V vector components, curr. currents, net OLR net outgoing longwave radiation, net heat balance of components, Euph Z euphotic depth or water clarity, optical dust extinction, Ek V Northward Ekman transport, and net solar radiation.

trade winds (-U) draw low saline water from the Caribbean during high tides.

Wavelet spectral analysis (not shown) found significant oscillations at ~ 3.5 year for sea level and zonal wind, and ~ 7 year periods for CHLa and salinity. These rhythms derive from the Atlantic Walker Circulation (Jury & Nieves Jiménez, 2020). A striking feature in Fig. 9B, Fig. 9C is the downtrend in U wind and salinity since 2016 and sustained high tides since 2018. Increased Northward Ekman transport is linked to faster Atlantic trade winds and account for the uptick in bioluminescent dinoflagellates after 2017.

To characterize spatial patterns of inter-annual variability, the chlorophyll time series was regressed onto Aug-Nov environmental fields 2002-2022 (Fig. 9D, Fig. 9E). A N-S dipole pattern emerges: phytoplankton blooms relate to weaker trade winds / warmer SST in the Caribbean, and stronger trade winds/cooler SST in the Atlantic. Aug-Nov chlorophyll concentrations at Fajardo are stimulated by Northward currents off the East coast of Puerto Rico that entrain Caribbean waters (Fig. 9E). The N-S dipole pattern and trends (cf. Fig. 9B, Fig. 9C) suggest a Northward expansion of trade winds consistent with climate change impacts.

Hurricanes: Northeastern Puerto Rico experienced eight tropical cyclones during the

field campaign 2016-2021; hurricanes in 2017 impacted the LGF environment via 6 m waves, 0.8 m tidal surge, and 32 m/s winds that stripped vegetation (Fig. 10A, Fig. 10B, Fig. 10C). Hurricane Maria changed structural and functional features in the lagoon. It dropped local SST from 30.5° to 28.3° C and salinity from 35.5 ‰ to 34.4 ‰ in Sep 2017, creating thermodynamic conditions for dinoflagellate blooms in LGF - following recovery from initial mechanical stress (Fig. 1D and Fig. 2B).

DISCUSSION

During this study we found widely fluctuating dinoflagellate densities at LGF: rising in late summer and declining in late winter, similar to seasonal patterns of *P. bahamense* in Tampa Bay, where sea temperatures modulate cyclical blooms. The greatest dinoflagellate densities at LGF coincided with high tides and low salinity from Aug-Nov. While our short-term monitoring uncovered frequent and intense blooms in 2018-2021, (Hinder et al., 2012) found a down-trend of dinoflagellate densities in the Northeast Atlantic due to increasing SST and wind speed. That study challenged the view that algal blooms are on the rise and found that previously abundant dinoflagellates *C. furca* and *Protoperidinium*

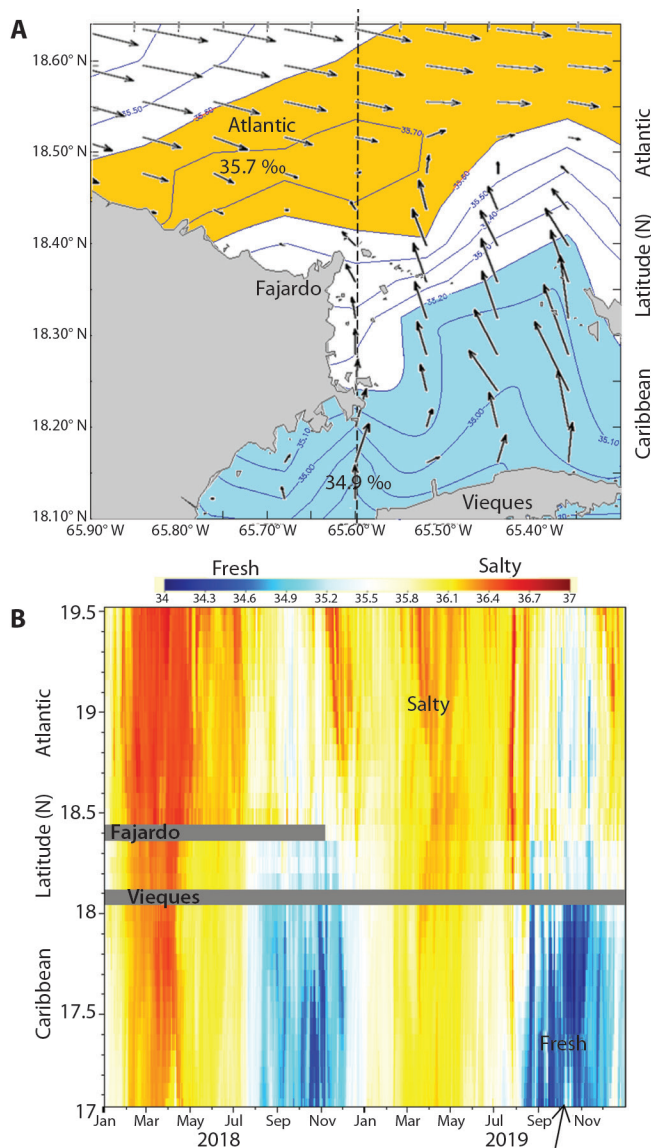


Fig. 8. A. Hycom surface currents (vector largest 0.2 m/s) and salinity (‰) on 10 Oct 2019 during a dinoflagellate bloom in LGF. **B.** Hycom surface salinity hovmöller plot N-S on 65.6W off Fajardo in 2018-19, arrow identifies map date.

spp. have diminished. Pre-hurricane results at LGF showed a similar effect, when stakeholders reported bioluminescent ‘blackouts’. After the storm surges in 2017, our study found sustained blooms that boosted eco-tourism.

Similarly, Hurricanes of 2017 in Florida’s coastal waterways caused enhanced nutrient loads which drove *P. bahamense* blooms in the

Indian River Lagoon and Lake Okeechobee (Philips, 2020). This study reported blooms immediately after Hurricanes due to exceptionally high rainfall resulting from large inflows of nutrient-rich water to the waterbodies through increases in dissolved inorganic nitrogen, intense re-suspension of muddy flocculent bottom sediments, resulting in high total

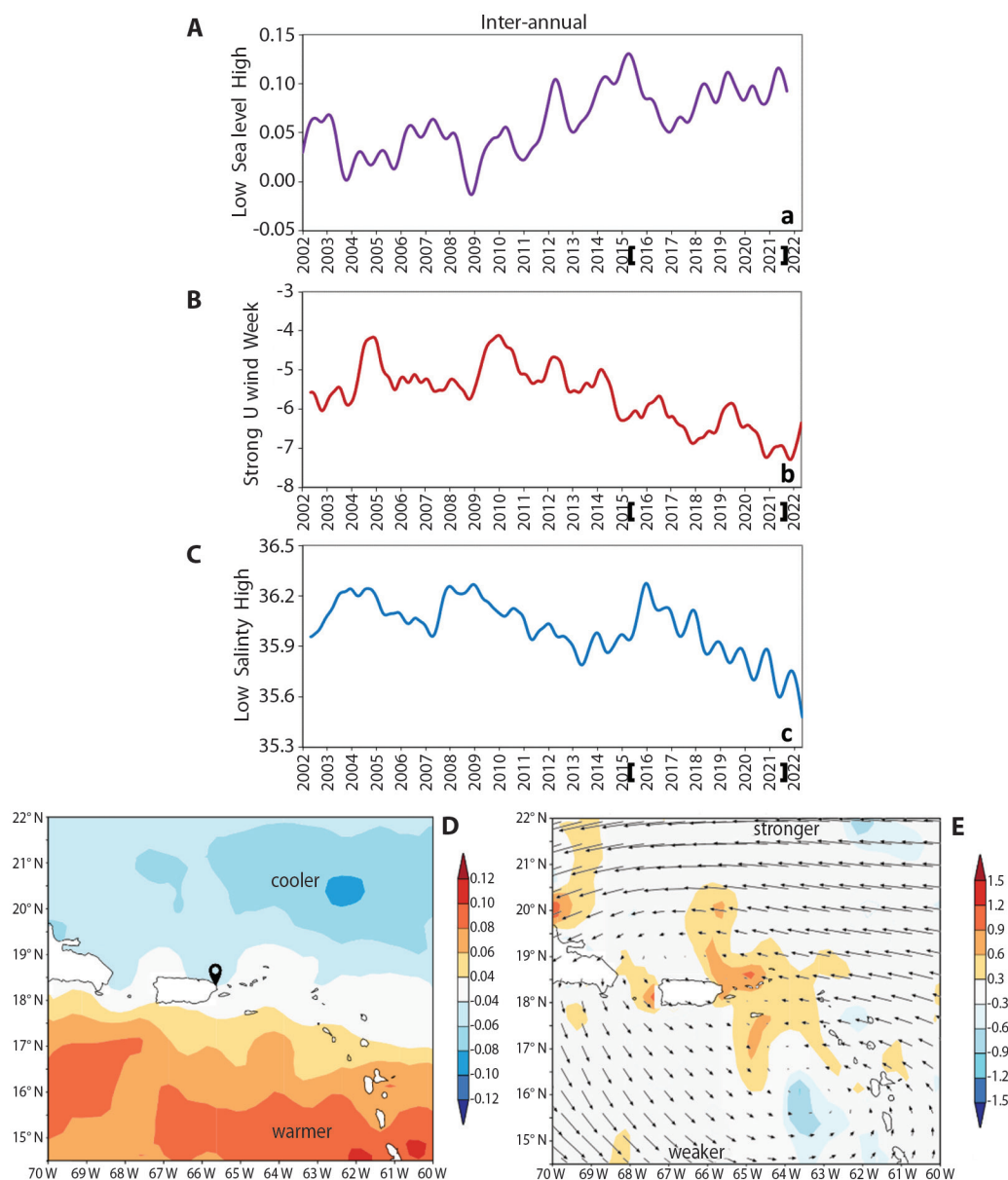


Fig. 9. Inter-annual filtered satellite reanalysis time series at Fajardo: **A.** Sea level. **B.** U wind. **C.** salinity, with field monitoring bracketed, annual tick marks on July. Inter-annual regression of CHLa time series onto Aug–Nov fields 2002–2022: **D.** SST (shaded /°C) Fajardo , and **E.** meridional current (shaded + Northward, /m s⁻¹) and wind (vector anomalies, largest 2 m/s).

suspended solids concentrations and increased nutrient concentrations through sediment re-suspension and re-mineralization of nutrients from damaged aquatic vegetation (e.g. sea-grasses) and damaged terrestrial biomass in the watershed. These key processes were also

observed in LGF following Hurricanes Irma and Maria explaining the *P. bahamense* in the following years, i.e. 2018 and 2019.

Increased sea level and lower salinity favored dinoflagellate growth in the longer-term, and these two are linked (Fig. 11A).

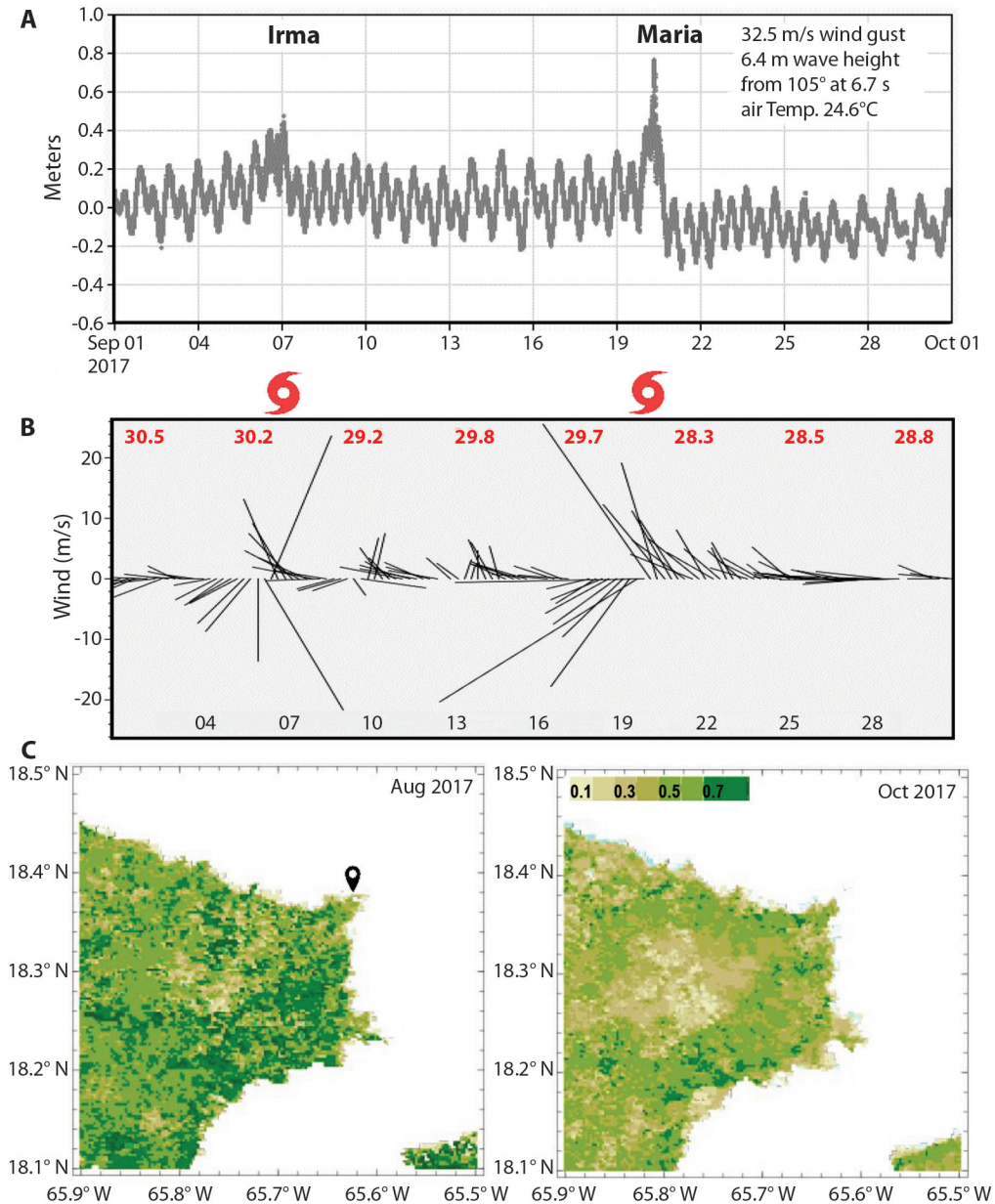


Fig. 10. A. Fajardo gauge sea level during Sep 2017 hurricanes; inset: buoy data at Maria landfall 20 Sep 2017. B. Daily wind stick vectors during Sep 2017 and buoy SST (red labels). C. Before (left) and after changes in satellite vegetation color.

Given that plumes of seawater come from the Orinoco and Amazon Rivers; the salinity budget depends on the relative flux of Caribbean versus Atlantic seawater. Tropical climate patterns modulate Fajardo daily sea level, as evidenced by regression onto Aug-Nov fields of

netOLR 2002-2022 (Fig. 11B) which show that a dry climate in the East Pacific contributes to high tides which support bioluminescence.

The late summer peak in dinoflagellate counts at LGF is like the higher latitudes (Hinder et al., 2012; Marcinko et al., 2013, Lopez et

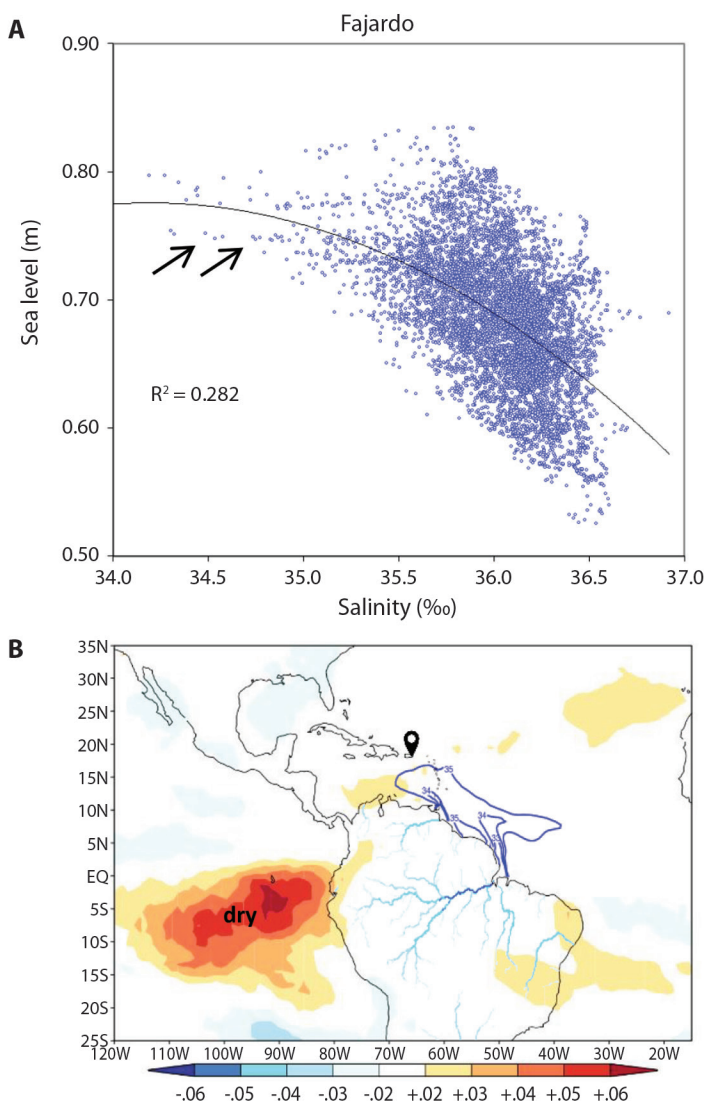


Fig. 11. A. Scatterplot of daily EC sea level and HYCOM salinity 2002-2022 and regression fit; arrows point to conditions favoring bioluminescence in LGF. **B.** Regression of daily sea level at Fajardo onto Aug-Nov 2002-2022 field of net OLR ($W m^{-2}$). South American river discharge and plume edge shown by blue contours $> 1000 m^3/s$ (land) and $< 35‰$ (sea).

al., 2021). Light winds and mixed layer response to seasonal heating promote algal blooms. Naturally these macro-scale studies do not capture local effects such as the dip in LGF dinoflagellates during mid-summer, when strong Easterly winds bring Saharan dust plumes (Angeles et al., 2010; Jury & Nieves Jiménez, 2020).

The environmental health of tidal lagoons is vital to coastal tourism and ongoing resource

management. Our LGF results revealed that: 1) dinoflagellate counts fluctuate widely—often surprising our monitoring team, 2) bioluminescent dinoflagellates are sensitive to small changes in environmental conditions—subtropical islands experience limited seasonality so biota have a narrow physiological range and few opportunities to adapt, 3) hurricanes ‘rake and refresh’ the marine environment for subsequent



bioluminescent blooms following recovery—an inference requiring further data, and 4) intra-seasonal fluctuations of LGF dinoflagellate density relate to ocean-atmosphere thermodynamic conditions, the salinity budget and sea level. We recommend continued monthly in-situ monitoring of LGF biota and on-going support for marine observations to guide conservation strategies of this natural resource, amidst a changing climate.

Ethical statement: the authors declare that they all agree with this publication and made significant contributions; that there is no conflict of interest of any kind; and that we followed all pertinent ethical and legal procedures and requirements. All financial sources are fully and clearly stated in the acknowledgments section. A signed document has been filed in the journal archives.

ACKNOWLEDGMENTS

Project funding was provided by Para la Naturaleza and Interamerican University of Puerto Rico, Institutional Funds. The authors acknowledge family, students, and colleagues who collected and processed samples in the Climate and Ecological Studies Laboratory from 2016 to 2021. Websites used in our data analysis include Climate Explorer KNMI, IRI Climate Library, University of Hawaii APDRC, NOAA NDBC.

REFERENCES

- Álvarez, S., Brown, C. E., García Díaz, M., O'Leary, H., & Solís, D. (2024). Non-linear impacts of harmful algae blooms on the coastal tourism economy. *Journal of Environmental Management*, 351, 119811. <https://doi.org/10.1016/j.jenvman.2023.119811>
- Angeles, M. E., González, J. E., Ramírez-Beltrán, N. D., Tepley, C. A., & Comarazamy, D. E. (2010). Origins of the Caribbean rainfall bimodal behavior. *Journal of Geophysical Research: Atmospheres*, 115(D11106). <https://doi.org/10.1029/2009jd012990>
- Badyalak, S., & Phlips, E. J. (2009). *Pyrodinium Bahamense* one the most significant harmful https://www.researchgate.net/publication/330565577_Pyrodinium_bahamense_One_the_Most_Significant_Harmful_Dinoflagellate_in_Mexico
- Balmaseda, M. A., Hernandez, F., Storto, A., Palmer, M. D., Alves, O., Shi L., Smith, G. C., Toyoda, T., Valdivieso, M., Barnier, B., Behringer, D., Boyer, T., Chang, Y. S., Chepurin, G. A., Ferry, N., Forget, G., Fujii, Y., Good, S., Guinehut, S., & Gaillard, F. (2015). The Ocean Reanalyses Intercomparison Project (Ora-IP). *Journal of Operational Oceanography*, 8(sup1). <https://doi.org/10.1080/1755876x.2015.1022329>
- CariCOOS (1996). *NDBC station page. National Data Buoy Center*. https://www.ndbc.noaa.gov/station_page.php?station=41056
- Chassignet, E., Hurlburt, H., Metzger, E. J., Smedstad, O., Cummings, J., Halliwell, G., Bleck, R., Baraille, R., Wallcraft, A., Lozano, C., Tolman, H., Srinivasan, A., Hankin, S., Cornillon, P., Weisberg, R., Barth, A., He, R., Werner, F., & Wilkin, J. (2009). US GODAE: Global ocean prediction with the hybrid coordinate ocean model (HYCOM). *Oceanography*, 22(2), 64–75. <https://doi.org/10.5670/oceanog.2009.39>
- Chawla, A., Tolman, H. L., Gerald, V., Spindler, D., Spindler, T., Alves, J. G. M., Cao, D., Hanson, J. L., & Devaliere, E. (2013). A multigrid wave forecasting model: A new paradigm in operational wave forecasting. *Weather and Forecasting*, 28(4), 1057–1078. <https://doi.org/10.1175/WAF-D-12-00007.1>
- Department of Environment and Natural Resources. (2013). Comunicado de Prensa DRNA Y JCA revelan resultados sobre laguna bioluminiscente de Fajardo. <https://www.drna.pr.gov/wp-content/uploads/2019/10/r-CP-6-de-diciembre-de-2013-DRNA-y-JCA-revelan-resultados-sobre-laguna-bioluminiscente-de-Fajardo.pdf>
- Fiorendino, J. M., Gaonkar, C. C., Henrichs, D. W., & Campbell, L. (2021). Drivers of microplankton community assemblage following tropical cyclones. *Journal of Plankton Research*, 45(1), 205–220. <https://doi.org/10.1093/plankt/fbab073>
- Hersbach, H., Bell, B., Berrisford, P., Hirahara, S., Horányi, A., Muñoz-Sabater, J., Nicolas, J., Peubey, C., Radu, R., Schepers, D., Simmons, A., Soci, C., Abdalla, S., Abellan, X., Balsamo, G., Bechtold, P., Biavati, G., Bidlot, J., Bonavita, M., ... & Thépaut, J. (2020). The ERA5 global reanalysis. *Quarterly Journal of the Royal Meteorological Society*, 146(730), 1999–2049. <https://doi.org/10.1002/qj.3803>
- Hinder, S. L., Hays, G. C., Edwards, M., Roberts, E. C., Walne, A. W., & Gravenor, M. B. (2012). Changes in marine dinoflagellate and diatom abundance under climate change. *Nature Climate Change*, 2(4), 271–275. <https://doi.org/10.1038/nclimate1388>

- Huber, N. (2012). *Estuaries -- Phytoplankton Protocol Washington*. <http://courses.washington.edu/uwtoce12/methods/sops/phytoplankton.pdf>
- Jury, M. R. (2020). Sand transport in the northeastern Caribbean characterized by wind-wave-current data. *Ocean & Coastal Management*, 198, 105363. <https://doi.org/10.1016/j.ocecoaman.2020.105363>
- Jury, M. R., & Nieves Jiménez, A. T. (2020). Tropical Atlantic dust and the zonal circulation. *Theoretical and Applied Climatology*, 143(3–4), 901–913. <https://doi.org/10.1007/s00704-020-03461-4>
- Lopez, C. B., Tilney, C. L., Muhlbach, E., Bouchard, J. N., Villac, M. C., Henschen, K. L., Markley, L. R., Abbe, S. K., Shankar, S., Shea, C. P., Flewelling, L., Garrett, M., Badylak, S., Philips, E. J., Hall, L. M., Lasi, M. A., Parks, A. A., Paperno, R., Adams, D. H., ... & Hubbard, K. A. (2021). High-resolution spatiotemporal dynamics of harmful algae in the Indian River Lagoon (Florida)—a case study of *aureoumbra lagunensis*, *Pyrodinium Bahamense*, and *pseudo-nitzschia*. *Frontiers in Marine Science*, 8. <https://doi.org/10.3389/fmars.2021.769877>
- Marcinko, C. L. J., Painter, S. C., Martin, A. P., & Allen, J. T. (2013). A review of the measurement and modelling of Dinoflagellate bioluminescence. *Progress in Oceanography*, 109, 117–129. <https://doi.org/10.1016/j.pocean.2012.10.008>
- Morquecho, L. (2019). *Pyrodinium bahamense* one the most significant harmful dinoflagellate in Mexico. *Frontiers in Marine Science*, 6, 1. <https://doi.org/10.3389/fmars.2019.00001>
- O'Connell, S., Martini, A., & Ku, T. (2007). The hydrodynamics and biogeochemistry of bioluminescent. <https://keckgeology.org/files/pdf/symvol/20th/puertorico/occonnell.pdf>
- Pagán, G. (2021). *Esfuerzo multisectorial para Atender Situación de emergencia en Laguna Bioluminiscente en Fajardo*. DRNA. <https://www.drna.pr.gov/noticias/esfuerzo-multisectorial-para-atender-situacion-de-emergencia-en-laguna-bioluminiscente-en-fajardo/>
- Philips, E. J., Badylak, S., Nelson, N. G., & Havens, K. E. (2020). Hurricanes, El Niño and harmful algal blooms in two sub-tropical Florida estuaries: Direct and indirect impacts. *Scientific Reports*, 10(1). <https://doi.org/10.1038/s41598-020-58771-4>
- Saha, S., Moorthi, S., Wu, X., Wang, J., Nadiga, S., Tripp, P., Behringer, D., Hou, Y.-T., Chuang, H., Iredell, M., Ek, M., Meng, J., Yang, R., Mendez, M. P., van den Dool, H., Zhang, Q., Wang, W., Chen, M., & Becker, E. (2014). The NCEP climate forecast system version 2. *Journal of Climate*, 27(6), 2185–2208. <https://doi.org/10.1175/jcli-d-12-00823.1>
- Sastre, M. P., Sánchez, E., Flores, M., Astacio, S., Rodríguez, J., Santiago, M., Olivieri, K., Francis, V., & Núñez, J. (2013). Population fluctuations of *Pyrodinium bahamense* and *Ceratium furca* (Dinophyceae) in Laguna Grande, Puerto Rico, and environmental variables associated during a three-year period. *Revista de Biología Tropical*, 61(4), 1799–1813.
- Soler-Figueroa, B. M., & Otero, E. (2014). The influence of rain regimes and nutrient loading on the abundance of two dinoflagellate species in a tropical bioluminescent bay, Bahía Fosforescente, La Parguera, Puerto Rico. *Estuaries and Coasts*, 38(1), 84–92. <https://doi.org/10.1007/s12237-014-9827-0>
- Soler-Figueroa, B. M., & Otero, E. (2016). Seasonal changes in bioluminescence and dinoflagellate composition in a tropical bioluminescent bay, Bahía Fosforescente, La Parguera, Puerto Rico. *Journal of Experimental Marine Biology and Ecology*, 483, 120–129. <https://doi.org/10.1016/j.jembe.2016.07.008>
- Soler-López, L. R., & Santos, C. R. (2010). *Selected hydrologic, water-quality, biological, and sedimentation characteristics of Laguna Grande, Fajardo Puerto Rico, March 2007-February 2009*. U.S. Geological Survey, Scientific Investigations Report 2010-5071.
- Storto, A., Alvera-Azcárate, A., Balmaseda, M. A., Barth, A., Chevallier, M., Counillon, F., Domingues, C. M., Drevillon, M., Drillet, Y., Forget, G., Garric, G., Haines, K., Hernandez, F., Iovino, D., Jackson, L. C., Lellouche, J.-M., Masina, S., Mayer, M., Oke, P. R., & Zuo, H. (2019). Ocean reanalyses: Recent advances and unsolved challenges. *Frontiers in Marine Science*, 6. <https://doi.org/10.3389/fmars.2019.00418>
- Tolman, H. L. (2002). *User manual and system documentation of WAVEWATCH III*. https://polar.ncep.noaa.gov/mmab/papers/t276/MMAB_276.pdf
- U.S. Geological Survey. (2021). *National Water Information System for Rio Fajardo, PR (river discharge data)*. water-data.usgs.gov/pr/nwis/uv?site_no=50070900
- Weaver, P.L., Ramirez, J. L., & Rivera, J. L.C. (1999). Las Cabezas de San Juan Nature Reserve. *Inception Report*, U.S. Dept. Agriculture, Washington D.C. (pp. 1–27).
- Xei, I. (2013). A puzzling “blackout” at Puerto Rico’s famous Bioluminescent Bay. <https://www.bloomberg.com/news/articles/2013-11-22/a-puzzling-blackout-at-puerto-rico-s-famous-bioluminescent-bay>